Polymer Journal (2020) 52:133–143
https://doi.org/10.1038/s41428-019-0272-6

ORIGINAL ARTICLE

Sequence-defined oligo/poly(ester-amide-ester)s via an orthogonal nucleophilic substitution reaction and a Passerini reaction

Yao-Zong Wang[1] · Jia-Chen Wang[1] · Yu-Huan Wu[1] · Chang-Xia Shi[1] · Fu-Sheng Du[1] · Zi-Chen Li[1]

Received: 25 June 2019 / Revised: 7 September 2019 / Accepted: 9 September 2019 / Published online: 30 September 2019

Abstract

We report the facile synthesis of sequence-defined, uniform oligo(ester-amide-ester)s, and periodic poly(ester-amide-ester)s composed of α-hydroxy acids and α-amino acids. The synthetic strategy for preparing the oligomers involves two sequential steps with bromoacetic acid and potassium isocyanoacetate as the key building blocks. (1) The first step is a nucleophilic substitution reaction between a bromoacetic ester and potassium isocyanoacetate to generate a new isocyanoacetic ester, (2) and the second is a Passerini reaction of the formed isocyanoacetic ester with an aldehyde and bromoacetic acid to form a longer bromoacetic ester with an ester-amide linkage and a side-group originating from the aldehyde. Repeating this cycle affords sequence-defined uniform oligo(ester-amide-ester)s with different side groups. This strategy efficiently provides uniform, symmetrical oligo(ester-amide-ester)s via an iterative approach. Furthermore, two strategies were examined to obtain sequence-defined periodic poly(ester-amide-ester)s through the polycondensation of different oligomers. The polycondensation based on the nucleophilic substitution of α,ω-bromo carboxylic acids as the oligomer was less effective, while the DIC/DPTS-mediated polycondensation of α,ω-hydroxy carboxylic acids as the sequence-defined oligomer was efficient enough to afford high-molecular-weight periodic poly(ester-amide-ester)s.

Introduction

Over the last two decades, great progress has been made in the design and synthesis of well-defined macromolecules with controlled architectures [1]. However, the manipulation of the polymer microstructure on a much smaller scale, for instance, controlling the monomer sequence, has only recently attracted adequate attention [2–5]. Today, many types of sequence-controlled polymers and sequence-defined, uniform oligomers have been synthesized by designing new monomers, controlling the polymerization kinetics, or using organic reaction-based iterative or exponential approaches [6–12]. Although not as powerful as biomacromolecules, sequence-defined synthetic polymers have been shown to have properties that are distinct from those of their random counterparts with identical compositions [13–15]. Ideally, for a sequence-defined polymer to behave more like a biomacromolecule, both the polymer backbone and the side-chain functionalities should be simple and well controlled [16–18]. Poly(ester-amide)s are promising materials that contain ester and amide linkages in their backbone [19–22]. This type of polymer shows good biodegradability due to the presence of ester linkages, and the occasional appearance of amide linkages gives the polymer with high thermal stability, good mechanical properties, and enhanced hydrophilicity and functionality. The simplest sequence-defined poly(ester-amide) is the alternating copolymer α-hydroxy acid and α-amino acid, which is generally synthesized via the ring-opening polymerization of dioxane-2,5-diones [19–22]. To determine how the inclusion of an isolated α-amino acid affects the properties of poly(ester-amide)s, we sought to

Supplementary information The online version of this article (https://doi.org/10.1038/s41428-019-0272-6) contains supplementary material, which is available to authorized users.

✉ Fu-Sheng Du
fsdu@pku.edu.cn

✉ Zi-Chen Li
zcli@pku.edu.cn

[1] Beijing National Laboratory for Molecular Sciences (BNLMS), Key Laboratory of Polymer Chemistry and Physics of Ministry of Education, Department of Polymer Science and Engineering, College of Chemistry and Molecular Engineering, Center for Soft Matter Science and Engineering, Peking University, 100871 Beijing, China

develop a synthetic platform for preparing longer sequence-defined poly(ester-amide)s composed of α-amino acids and α-hydroxy acids. As the first step, we focused our study on the synthesis of sequence-defined oligo(ester-amide-ester)s and periodic poly(ester-amide-ester) and the thermal properties of the resulting oligomers and polymers.

Our strategies for synthesizing uniform sequence-defined oligo(ester-amide-ester)s and periodic poly(ester-amide-ester)s composed of different α-hydroxy acids and α-amino acids are shown in Scheme 1. For the synthesis of uniform oligo(ester-amide-ester)s, the key is the utilization of two sequential orthogonal reactions: a nucleophilic substitution between a bromoacetic acid ester and potassium isocyanoacetate and a Passerini three-component reaction (P-3CR) between isocyanoacetate, bromoacetic acid, and an aldehyde [9, 22–24]. Thus, starting from *tert*-butyl bromoacetate and potassium isocyanoacetate, the nucleophilic substitution generates a new ester linkage, and the end group is transformed from an active bromide into an isocyanide. Using the advantage offered by the simultaneous in situ ester-amide linkage formation and side-chain functionality incorporation of P-3CR [22–24], we can introduce both backbone and side-chain sequences in the second step, and at the same time, the end group is converted back into an active bromide. By repeating these two sequential reactions with potassium isocyanoacetate, bromoacetic acid, and different aldehydes, uniform oligo(ester-amide-ester)s with a backbone sequence of α-hydroxy acid, α-amino acid, and α-hydroxy acid and ordered side chains from the aldehyde could be obtained. Alternatively, by replacing bromoacetic acid with boric acid in the P-3CR and then deprotecting the *tert*-butyl group, an α-hydroxyl and ω-carboxyl terminated oligo (ester-amide-ester) can be obtained. This compound can be polymerized to afford the corresponding periodic poly(ester-amide-ester)s.

Experimental

Materials

Tert-butyl bromoacetate (98%), ethyl isocyanoacetate (98%), phenylacetaldehyde (98%), isobutyraldehyde (98%), 10-undecenal (98%), 1,3- (DIC, 98%), and 4-(dimethylamino) pyridine (98%) were purchased from Alfa Aesar and used as received. Bromoacetic acid (98%), *p*-toluene sulfonic acid monohydrate (98%), trifluoroacetic acid (98%), triethylamine (AR), boric acid (AR), potassium hydroxide (AR), potassium carbonate (AR), and all other chemicals were purchased from Beijing Chem. Reagent Co. and were used as received unless otherwise noted. Potassium isocyanoacetate was obtained by hydrolysis of ethyl isocyanoacetate according to the literature method (Fig. S1) [25]. 4-(Dimethylamino) pyridinium p-toluene sulfonate (DPTS) was obtained by following a literature method [26].

Measurement

^{1}H NMR (400 MHz) spectra were recorded in $CDCl_3$, CD_3OD, or DMSO-d_6 at 25 °C on a Varian Gemini 400 spectrometer with tetramethylsilane as the internal reference for chemical shifts (δ, ppm). The molecular weights and dispersities ($Đ = M_w/M_n$) of the polymers were measured by gel permeation chromatography (GPC) on an instrument equipped with a 2414 refractive index detector, a Waters 1525 binary HPLC pump, and three Waters Styragel HT columns (HT2, HT3, and HT4). The columns were thermostated at 35 °C, and THF was used as the eluent at a flow rate of 1.0 mL/min. The system was calibrated against standard linear polystyrenes.

Polymer **P1** was fractionated into three samples with different molecular weights and narrow dispersities with a

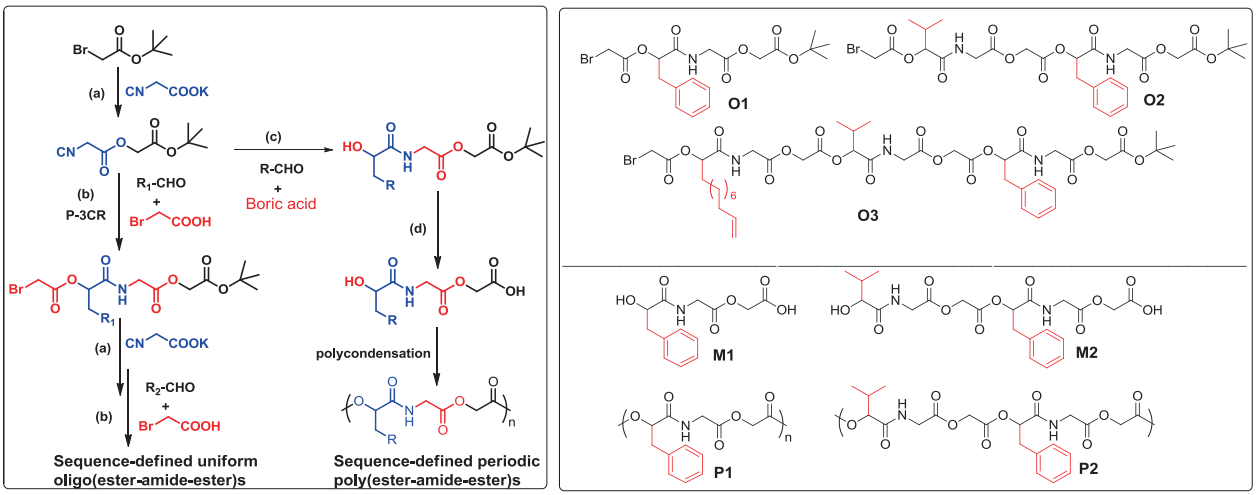

Scheme 1 Synthesis of sequence-defined oligo/poly(ester-amide-ester)s

recycling preparative GPC (JAI LaboACE LC-5060) equipped with two JAIGEL HR columns (2 HR and 2.5 HR), a UV detector, and an RI detector. Chloroform containing 0.05% ethanol was used as the eluent at a flow rate of 8.0 mL/min.

Electrospray ionization (ESI) mass spectra were obtained on a Bruker Apex IV mass spectrometer in positive ion mode. Matrix-assisted laser desorption ionization time-of-flight (MALDI-TOF) mass spectra were obtained on a Bruker Autoflex III mass spectrometer equipped with a 355 nm nitrogen laser. α-Cyano-4-hydroxycinnamic acid was used as the matrix, and linear positive ion mode was used.

Thermal gravimetric analysis (TGA) was carried out using a Q600-SDT thermogravimetric analyzer (TA Co., Ltd.) with a nitrogen purging rate of 50 mL/min. Measurements were taken from room temperature to 600 °C at a heating rate of 10 °C/min. Calorimetric measurements were made using a Q100 differential scanning calorimeter (TA Co., Ltd.) with a nitrogen purging rate of 50 mL/min. The program was set to conduct two cycles of heating and cooling over a temperature range of −80 °C to the desired temperature (50 °C below T_d) at a heating/cooling rate of 10 °C/min. The data for constructing the endothermic curve were acquired from the second scan. TA Universal Analysis software was employed for data acquisition and processing.

General procedure for the nucleophilic substitution reaction

To a solution of bromoacetic acid ester (10 mmol) in DMF (40 mL, 0.25 M) was added potassium isocyanoacetate (11 mmol). The heterogeneous suspension was stirred at room temperature for 3 h. After filtration to remove the formed salt, DMF was removed via evaporation under reduced pressure. The viscous solution was then diluted with CH_2Cl_2 and washed with brine three times to remove the residual salt. The organic phases were combined, dried over sodium sulfate, and concentrated to give the corresponding isocyanides, which were used directly in the next step.

Isocyanide **I1**: Viscous, yellow oil, 87% yield.

^{1}H NMR (400 MHz, $CDCl_3$), δ (ppm) (Fig. S2A): 4.62 (s, 2H), 4.39 (s, 2H), 1.48 (s, 9H).

Isocyanide **I2**: Viscous, yellow oil, 92% yield.

^{1}H NMR (400 MHz, $CDCl_3$), δ (ppm) (Fig. S2B): 7.34–7.14 (m, 5H), 6.65–6.53 (br, 1H), 5.50 (dd, $J = 7.2$, 4.6 Hz, 1H), 4.76 (d, $J = 15.9$ Hz, 1H), 4.68 (d, $J = 15.8$ Hz, 1H), 4.55 (s, 2H), 4.30 (s, 2H), 4.12 (s, 1H), 4.11 (s, 1H), 3.27 (dd, $J = 14.5$, 4.9 Hz, 1H), 3.17 (dd, $J = 14.4$, 7.2 Hz, 1H), 1.47 (s, 9H).

Isocyanide **I3**: Viscous, pale-yellow oil, 86% yield.

^{1}H NMR (400 MHz, $CDCl_3$), δ (ppm) (Fig. S2C): 7.36–7.13 (m, 5H), 6.77–6.63 (br, 2H), 5.50 (dd, $J = 7.2$, 4.6 Hz, 1H), 5.14 (d, $J = 4.4$, 1H), 4.84 (s, 2H), 4.65 (s, 2H), 4.55 (s, 2H), 4.38 (s, 2H), 4.24–3.99 (m, 4H), 3.27 (dd, $J = 14.4$, 4.4 Hz, 1H), 3.16 (dd, $J = 14.4$, 7.2 Hz, 1H), 2.39–2.26 (m, 1H), 1.48 (s, 9H), 0.99 (d, $J = 6.8$ Hz, 3H), 0.97 (d, $J = 8.0$ Hz, 3H).

General procedure for the P-3CR

To a suspension of the appropriate aldehyde (10 mmol) and isocyanide (10 mmol) in water (40 mL) was added bromoacetic acid (10 mmol) [27]. The heterogeneous mixture was stirred at room temperature for 24 h. The organic phase was then separated, and the aqueous phase was extracted with CH_2Cl_2 three times. The combined organic phase was dried over sodium sulfate, and the CH_2Cl_2 was removed via evaporation. The crude product was purified by either recrystallization or silica gel column chromatography.

Oligo(ester-amide-ester) **O1**: Recrystallized from petroleum ether/ethyl acetate mixture, pale-yellow powder, 56% yield.

^{1}H NMR (400 MHz, $CDCl_3$), δ (ppm) (Fig. 1a): 7.32–7.17 (m, 5H), 6.68–6.62 (br, 1H), 5.48 (dd, $J = 7.8$, 4.4 Hz, 1H), 4.55 (s, 2H), 4.16 (dd, $J = 18.2$, 5.2 Hz, 1H), 4.10 (dd, $J = 18.2$, 5.2 Hz, 1H), 3.84 (d, $J = 12.4$ Hz, 1H), 3.78 (d, $J = 12.3$ Hz, 1H), 3.30 (dd, $J = 14.4$, 4.4 Hz, 1H), 3.15 (dd, $J = 14.4$, 7.8 Hz, 1H), 1.47 (s, 9H).

ESI-MS (m/z): $[M + NH_4]^+$ calcd for $C_{19}H_{28}N_2O_7Br$ (Fig. S5): 475.1, 477.1, found: 475.1, $[M + K]^+$ calcd for $C_{19}H_{24}NO_7BrK$: 496.0, 498.0, found: 496.0.

Oligo(ester-amide-ester) **O2**: purified by silica gel column chromatography (petroleum ether/ethyl acetate, v/v = 1/3), white powder, 77% yield.

^{1}H NMR (400 MHz, $CDCl_3$), δ (ppm) (Fig. 1b): 7.33–7.14 (m, 5H), 6.82–6.69 (br, 2H), 5.53–5.47 (m, 1H), 5.12 (d, $J = 4.4$ Hz, 1H), 4.64 (s, 2H), 4.55 (s, 2H), 4.22–3.98 (m, 4H), 3.93 (s, 2H), 3.31–3.23 (m, 1H), 3.16 (dd, $J = 14.4$, 7.4 Hz, 1H), 2.39–2.27 (m, 1H), 1.47 (s, 9H), 1.01 (d, $J = 2.3$ Hz, 3H), 0.99 (d, $J = 2.8$ Hz, 3H).

ESI-MS (m/z): $[M + H]^+$ calcd for $C_{28}H_{38}N_2O_{12}Br$ (Fig. S6): 673.2, 675.2, found: 673.2, $[M + Na]^+$ calcd for $C_{28}H_{37}N_2O_{12}BrNa$: 695.1, 697.1, found: 697.1, $[M + K]^+$ calcd for $C_{28}H_{37}N_2O_{12}BrK$: 711.1, 713.1, found: 713.1.

Oligo(ester-amide-ester) **O3**: white powder, 41% yield.

^{1}H NMR (400 MHz, $CDCl_3$), δ (ppm) (Fig. 1c): 7.34–7.15 (m, 5H), 6.89–6.71 (br, 3H), 5.80 (ddt, $J = 16.9$, 10.1, 6.7 Hz, 1H), 5.50 (dd, $J = 7.6$, 4.6 Hz, 1H), 5.24 (dd, $J = 7.3$, 4.8 Hz, 1H), 5.18–5.14 (m, 1H), 4.99 (dd, $J = 17.0$, 1.9 Hz, 1H), 4.95–4.90 (m, 1H), 4.77 (s, 2H), 4.65 (s, 2H), 4.55 (s, 2H), 4.22–4.01 (m, 6H), 3.93 (d, $J = 12.2$ Hz, 1H), 3.88 (d, $J = 12.3$ Hz, 1H), 3.28 (dd, $J = 14.4$, 4.6 Hz, 1H), 3.16 (dd, $J = 14.3$, 7.7 Hz, 1H), 2.45–2.18 (m, 1H), 2.09–1.98 (m, 2H), 1.96–1.78 (m, 2H), 1.47 (s, 9H), 1.41–1.23 (m, 12H), 0.98 (d, $J = 6.4$ Hz, 3H), 0.96 (d, $J = 6.0$ Hz, 3H).

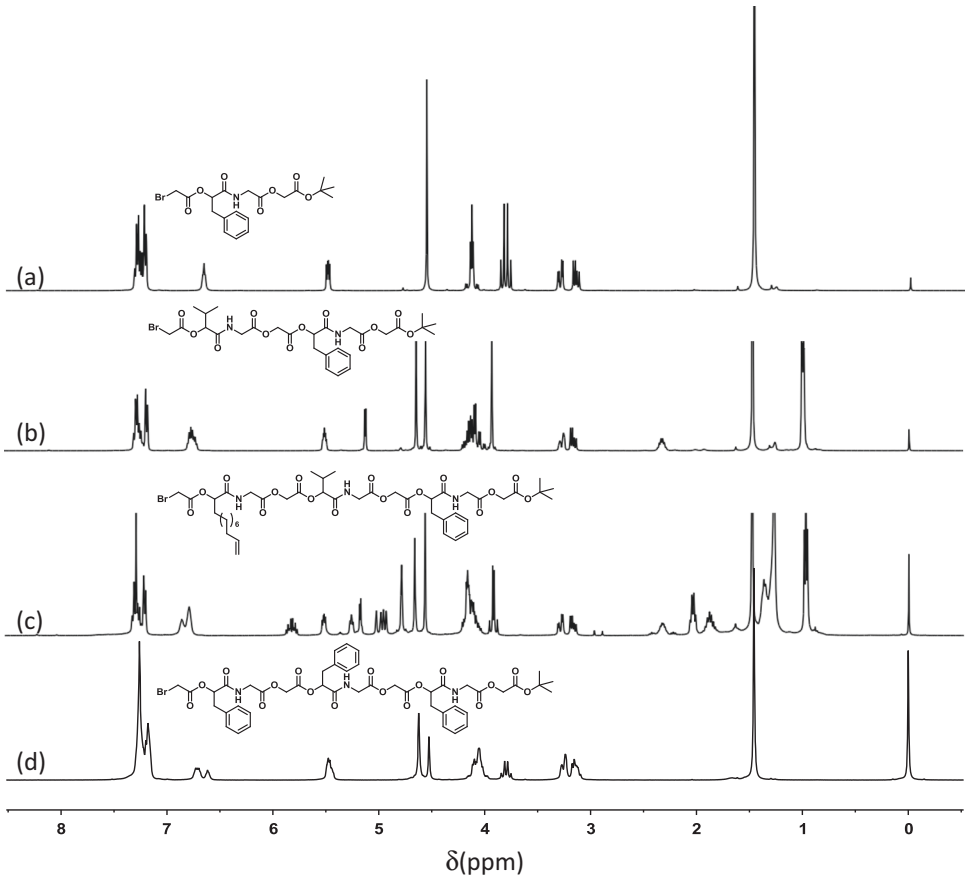

Fig. 1 ^{1}H NMR spectra of **a O1**, **b O2**, **c O3**, and **d O'3** in $CDCl_3$

ESI-MS (m/z): $[M + H]^+$ calcd for $C_{44}H_{63}N_3O_{17}Br$ (Fig. S7): 984.3, 986.3, found: 986.3.

Oligo(ester-amide-ester) **O′3**: white solid, 60% yield.

^{1}H NMR (400 MHz, $CDCl_3$), δ (ppm) (Fig. 1d): 7.36–7.11 (m, 15H), 6.78–6.57 (br, 3H), 5.52–5.40 (m, 3H), 4.62 (s, 4H), 4.53 (s, 2H), 4.17–3.96 (m, 6H), 3.83 (d, J = 12.4 Hz, 1H), 3.77 (d, J = 12.4 Hz, 1H), 3.31–3.21 (m, 3H), 3.19–3.08 (m, 3H), 1.46 (s, 9H).

ESI-MS (m/z): $[M + NH_4]^+$ calcd for $C_{45}H_{54}N_4O_{17}Br$ (Fig. S8): 1001.3, 1003.3, found: 1003.3.

General procedure for the boric acid-mediated Passerini reaction

To a solution of the appropriate aldehyde (10 mmol) and isocyanide (10 mmol) in DMF (40 mL) was added boric acid (10 mmol) [28]. The homogeneous solution was stirred at room temperature for 24 h. The DMF was removed via evaporation under reduced pressure. The viscous residue was then diluted with CH_2Cl_2 and washed with brine three times to remove the salt and residual DMF. The organic layer was dried over sodium sulfate and concentrated to give the crude product.

α-Hydroxy-ω-*tert*-butyl ester **H1** was obtained as a white solid in 50% yield after recrystallization from petroleum ether/ethyl acetate.

^{1}H NMR (400 MHz, $CDCl_3$), δ (ppm) (Fig. S9A): 7.35–7.22 (m, 5H), 7.13–7.08 (br, 1H), 4.55 (s, 2H), 4.34 (dd, J = 8.9, 3.8 Hz, 1H), 4.18 (dd, J = 18.4, 5.7 Hz, 1H), 4.11 (dd, J = 18.4, 5.5 Hz, 1H), 3.25 (dd, J = 14.0, 3.8 Hz, 1H), 2.87 (dd, J = 14.0, 8.8 Hz, 1H), 2.83–2.74 (br, 1H), 1.47 (s, 9H).

α-Hydroxy-ω-*tert*-butyl ester **H2** was obtained as a white powder in 60% yield after purification by silica gel column chromatography (petroleum ether/ethyl acetate = 3:7).

^{1}H NMR (400 MHz, $CDCl_3$), δ (ppm) (Fig. S9B): 7.35–7.08 (m, 5H), 6.84–6.72 (br, 2H), 5.55–5.50 (m, 1H), 4.71–4.57 (m, 2H), 4.56 (s, 2H), 4.25–3.94 (m, 5H), 3.30–3.23 (m, 1H), 3.21–3.12 (m, 1H), 2.22–2.09 (m, 1H), 1.48 (s, 9H), 1.03 (d, J = 6.9 Hz, 3H), 0.87 (d, J = 6.8 Hz, 3H).

General procedure for deprotection of the *tert*-butyl ester group

Using the synthesis of monomer **M′1** as an example, compound **O1** was dissolved in a mixture of CH_2Cl_2 and trifluoroacetic acid (v/v = 3:1, 0.25 M). After stirring at

room temperature for 3 h, the solvent was removed by evaporation. The remaining viscous oil was diluted with ethyl acetate and washed with brine three times to remove the residual trifluoroacetic acid. The organic layer was dried over sodium sulfate and concentrated to afford **M′1** as a white powder in 81% yield.

^{1}H NMR (400 MHz, CD_3OD), δ (ppm) (Fig. S11): 7.30–7.18 (m, 5H), 5.34 (dd, $J = 8.3$, 4.4 Hz, 1H), 4.66 (s, 2H), 4.09 (d, $J = 17.7$ Hz, 1H), 4.02 (d, $J = 17.7$ Hz, 1H), 3.97 (s, 2H), 3.22 (dd, $J = 14.3$, 4.4 Hz, 1H), 3.10 (dd, $J = 14.3$, 8.3 Hz, 1H).

Monomer **M1** was synthesized from **H1** and recrystallized from petroleum ether/ethyl acetate. White crystals, 63% yield.

^{1}H NMR (400 MHz, DMSO-d_6), δ (ppm) (Fig. 2a): 8.24–8.17 (br, 1H), 7.34–7.15 (m, 5H), 4.60 (s, 2H), 4.11 (dd, $J = 8.9$, 3.5 Hz, 1H), 3.94 (d, $J = 2.8$ Hz, 1H), 3.93 (d, $J = 2.9$ Hz, 1H), 3.00 (dd, $J = 13.9$, 3.5 Hz, 1H), 2.69 (dd, $J = 13.9$, 8.9 Hz, 1H).

Monomer **M2** was synthesized from **H2** and purified by precipitation from diethyl ether. White crystals, 53% yield.

^{1}H NMR (400 MHz, DMSO-d_6), δ (ppm) (Fig. 2b): 8.69–8.62 (br, 1H), 8.14–8.07 (br, 1H), 7.33–7.19 (m, 5H), 5.26 (dd, $J = 8.6$, 4.0 Hz, 1H), 4.83–4.75 (m, 1H), 4.69–4.61 (m, 1H), 4.61 (s, 2H), 4.00–3.84 (m, 4H), 3.72 (d, $J = 3.5$ Hz, 1H), 3.13 (dd, $J = 14.4$, 4.1 Hz, 1H), 2.99 (dd, $J = 14.3$, 8.6 Hz, 1H), 2.04–1.92 (m, 1H), 0.91 (d, $J = 6.9$ Hz, 3H), 0.78 (d, $J = 6.8$ Hz, 3H).

General procedure for polymerization via nucleophilic substitution

To a solution of **M′1** (201.1 mg, 0.5 mmol) in DMF (1 mL) was added potassium carbonate (82.9 mg, 0.6 mmol). The

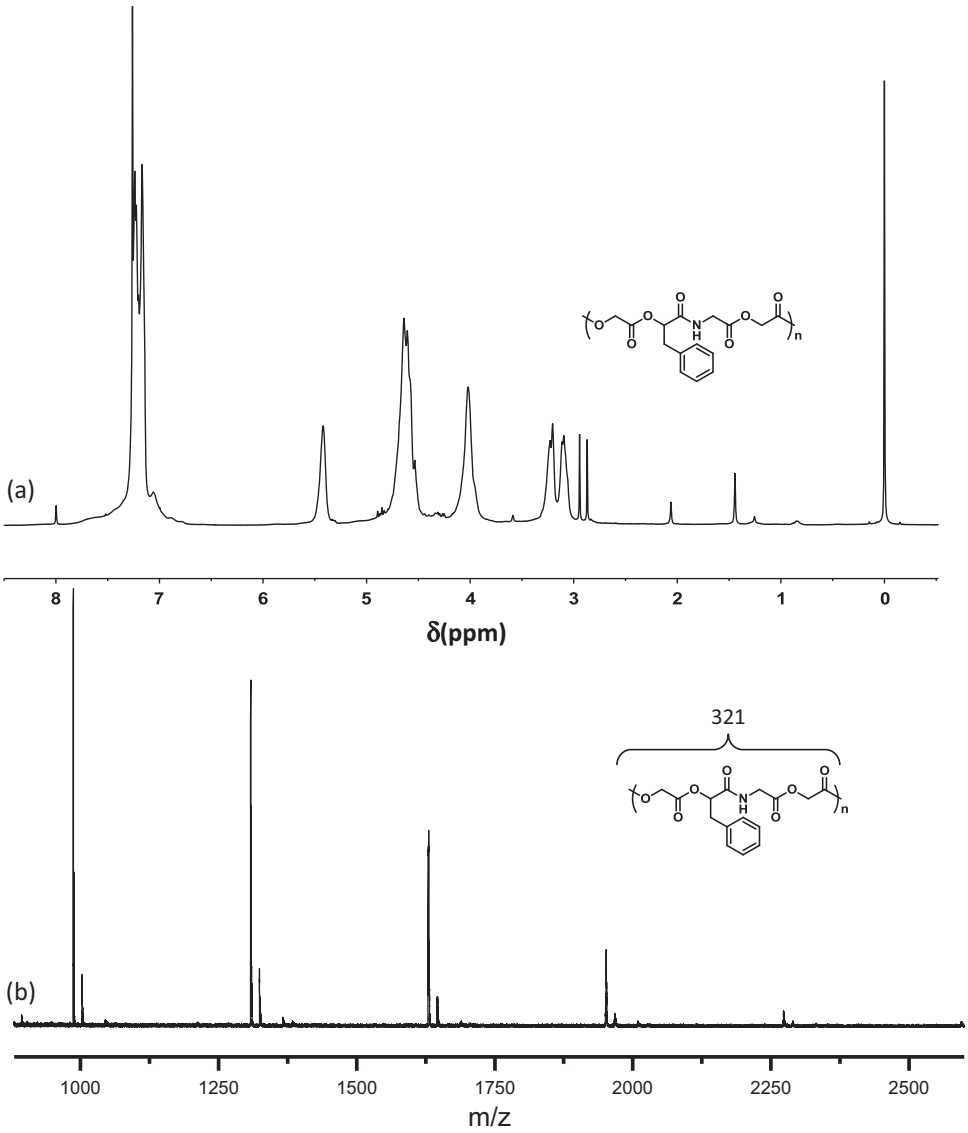

Fig. 2 ^{1}H NMR and MALDI-TOF-MS spectra of **P′1**

mixture was stirred at room temperature for 4 h and then diluted with CH_2Cl_2. The salt was removed by centrifugation. Afterward, the supernatant was concentrated and precipitated into diethyl ether three times to afford **P′1** as a white solid in 90% yield.

General procedure for DIC/DPTS-mediated polycondensation

Taking the polycondensation of **M1** as an example, **M1** (281.3 mg, 1.0 mmol) and DPTS (58.9 mg, 0.2 mmol) were dissolved in a mixture of CH_2Cl_2 (2 mL) and pyridine (0.1 mL). Once the solution was homogenized under gentle warming, DIC (189.3 mg, 1.5 mmol) was added under vigorous stirring. After stirring at room temperature for 24 h, the mixture was precipitated into methanol three times to remove the urea and give **P1** as a white solid in 48% yield.

P2 was synthesized from **M2** and obtained as a white solid in 43% yield.

Results and discussion

Synthesis of O1–O3 and O′3

The details of the synthetic route to **O1–O3** are shown in Scheme 2. The two reactions are efficient and orthogonal, and no additional protecting or deprotecting steps are needed. Thus, by repeating these two reactions with different aldehydes, oligo(ester-amide-ester)s with the desired side groups can be prepared. We started with the nucleophilic substitution reaction of potassium isocyanoacetate with *tert*-butyl bromoacetate. The carboxylic group at the chain end could provide an extra functional handle when unmasked. The substitution reaction was complete in ~3 h at room temperature. Simple filtration and concentration afforded isocyanide **I1** with sufficient purity. The structure of **I1** was confirmed by NMR spectroscopy (Figs. S2A and S3A). The methylene proton signals at 3.78 ppm for the *tert*-butyl bromoacetate (Br**CH$_2$**COO*t*Bu) shifted to 4.62 ppm (–COO–**CH$_2$**COO*t*Bu), and a new peak corresponding to the methylene protons adjacent to the isocyano group (CN–**CH$_2$**–COO–) appeared at 4.39 ppm, verifying the formation of the new ester linkage. To obtain oligomer **O1**, we initially conducted a P-3CR with compound **I1**, bromoacetic acid, and phenyl aldehyde in aprotic solvents, such as dichloromethane, chloroform, ethyl acetate, toluene, diethyl ether, and tetrahydrofuran, which are well-established as good solvents for P-3CR. The reaction was very slow, presumably due to the low reactivity of isocyanoacetate. Pirrung et al. reported that the P-3CR can be greatly accelerated by aqueous environments [27]. We therefore tested the reaction in water. The heterogeneous suspension was stirred at room temperature for 24 h, at which point complete conversion of isocyanoacetate was achieved. Pure **O1** was obtained in 56% yield after column chromatography and recrystallization. The structure of **O1** was confirmed by both NMR spectroscopy (Fig. 1a and Fig. S4A) and ESI MS (Fig. S5).

The above optimized reaction conditions were then used to synthesize **O2** and **O3**. Compound **O1** was reacted with potassium isocyanoacetate to obtain isocyanide **I2** (92% yield). Then, the P-3CR of **I2** with bromoacetic acid and isobutyraldehyde afforded **O2** (77% yield). Repeating the reaction of **O2** with potassium isocyanoacetate followed by P-3CR of formed **I3** with bromoacetic acid and 10-undecenal gave **O3**. Compounds **I2** and **I3** were

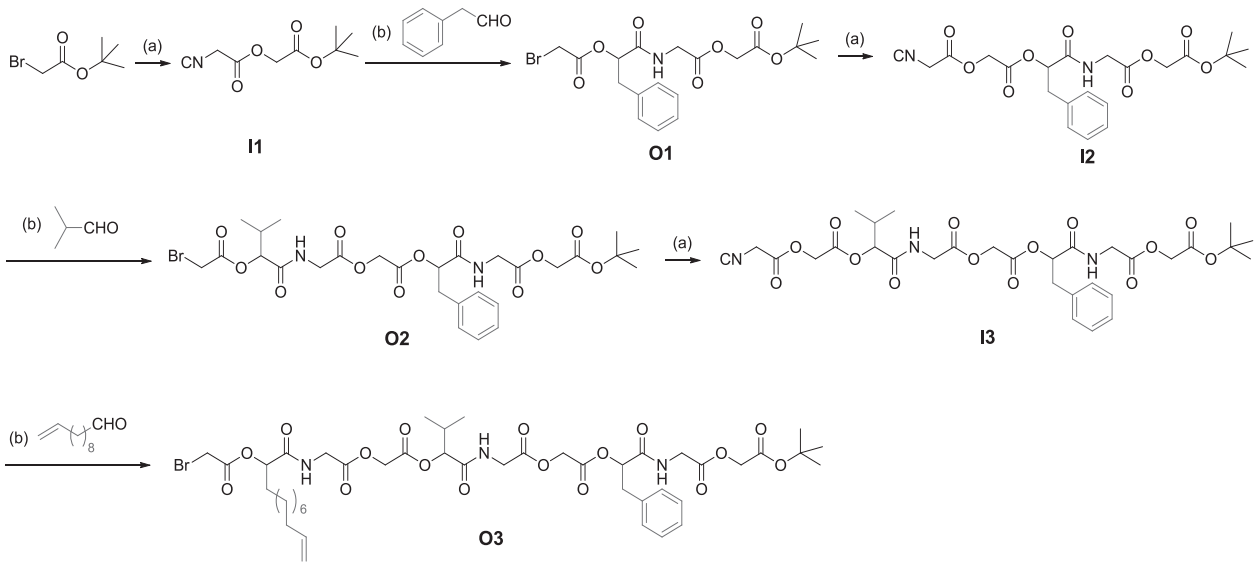

Scheme 2 Sequence-defined oligo(ester-amide-ester)s via a repeated two-step reaction approach. Reagents and conditions: (a) potassium isocyanoacetate, DMF, room temperature, 3 h; (b) bromoacetic acid, aldehyde, and water, room temperature, 24 h

characterized by NMR spectroscopy (Figs. S3 and S4). The structures of **O2** and **O3** were also confirmed by NMR spectroscopy (Fig. 1 and Fig. S4) and ESI MS (Figs. S6 and S7). We also used GPC to analyze the molecular weights of **O1**–**O3** (Fig. S13). The measured M_n values of **O1**, **O2**, and **O3** were 0.7, 1.1, and 1.6 kDa, respectively, and their dispersities all were close to 1.0 (Table 1).

To further enhance the synthetic efficiency, we expanded this synthetic strategy to an iterative process (Scheme 3). The *tert*-butyl ester group at the ω-chain end of **O1** could be quantitatively unmasked with trifluoroacetic acid, generating **M′1** as confirmed by its NMR spectra (Fig. S11). In addition, the α-chain end of **O1** could be equipped with an isocyano group by nucleophilic substitution with potassium isocyanoacetate to form **I2**. The P-3CR of **M′1**, phenylacetaldehyde, and **I2** generated **O′3**, which contains three pendant benzyl groups, and the structure of this compound was confirmed by NMR spectroscopy (Fig. 1d and Fig. S4D), ESI-MS (Fig. S8), and GPC (Fig. S13). It can be deduced that using **O′3** for further iterative processes would efficiently afford long-chain uniform oligomers with identical periodic repeating units, though at the cost of deprotecting one terminus.

Polymerization of sequence-defined oligo(ester-amide-ester)s

The advantage of the above approach is that we can obtain uniform oligo(ester-amide-ester)s with well-defined sequences. However, one inherent drawback is the difficulty

Table 1 Molecular weights and thermal data of the oligo/poly (ester-amide-ester)s

Oligomer/ Polymer	M_n (kDa)[a]	$Đ$[a]	T_d (°C)[b]	First stage weight loss (%)[b]		T_g (°C)[c]
				Experimental	Theoretical	
O1	0.7	1.03	174.6	12.15	12.24	1.6
O2	1.1	1.02	166.6	8.29	8.33	17.6
O3	1.6	1.02	175.0	5.76	5.70	22.4
O′3	1.5	1.02	178.5	5.58	5.70	37.0
P′1	5.5	1.50	228.5	–	–	75.9
P1	11.7	1.58	289.1	–	–	77.2
P2	11.1	1.22	255.4	–	–	90.4

[a]Determined by GPC using polystyrene calibrators

[b]Determined by TGA at a scan rate of 10 °C/min. T_d was defined as the temperature at 5% weight loss

[c]Determined by DSC at a scan rate of 10 °C/min. Values were determined from the second scan data

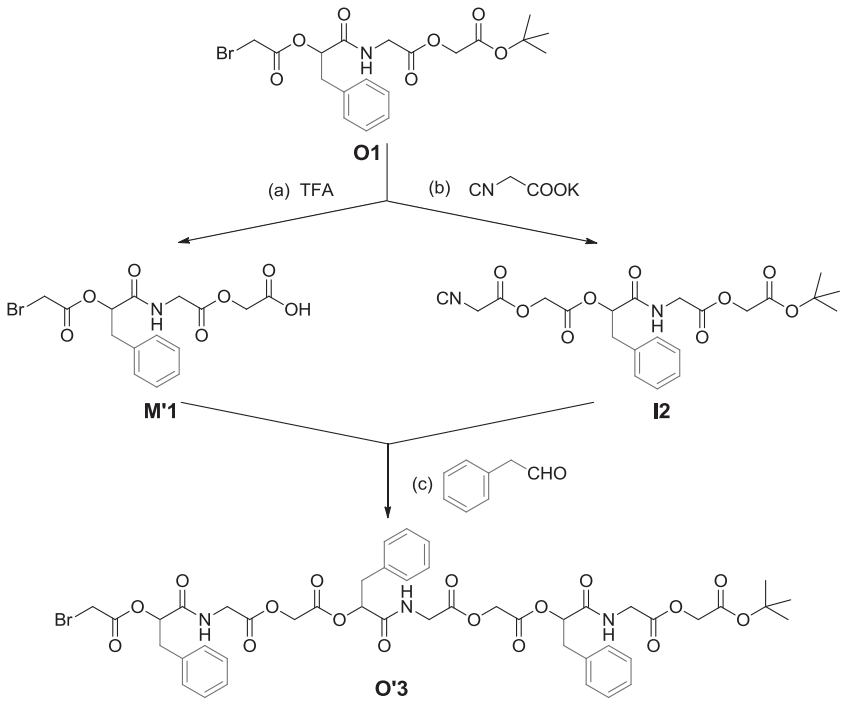

Scheme 3 Sequence-defined oligo(ester-amide-ester)s via an iterative approach. Reagents and conditions: **a** CH_2Cl_2/TFA (v/v = 3:1), room temperature, 3 h; **b** isocyanoacetate, DMF, room temperature, 3 h; and **c** phenylacetaldehyde and water, room temperature, 24 h

of practically obtaining high-molecular-weight polymers on a reasonable time scale. Thus, we decided to prepare monomers with similar defined sequences and then polymerize the monomers into sequence-defined periodic poly(ester-amide-ester)s (Scheme 4). Surely, these stepwise polymerizations will erode the monodispersity of the oligo(ester-amide-ester)s. Nevertheless, the purpose of this process was to seek a balance between structural precision and achieving sequence-defined polymers with a sufficiently high-molecular weight.

We tested two polymerization methods for generating periodic polymers from the corresponding α,ω-functionalized oligo(ester-amide-ester)s. Initially, monomer **M′1** was polymerized with potassium carbonate as a catalyst in DMF at room temperature for 4 h, and polymer **P′1** was obtained in 90% yield ($M_n = 5.5$ kDa and $Đ = 1.50$, Fig. S14). The structure of **P′1** was confirmed by NMR and MALDI-TOF-MS analyses (Fig. 2). The integrity of the polymer structure excluded the possible transesterification under these conditions. The molecular weight of **P′1** was only moderate due to the low efficiency of nucleophilic substitution reactions for polymerization.

To improve the polymerization result and obtain polymers with different sequences, another strategy based on the esterification of hydroxy groups with carboxylic acids was explored. As reported by Moore and Stupp [26], high-molecular-weight polyesters could be prepared from α,ω-hydroxy carboxylic acid monomers with 1,3-diisopropylcarbodiimide (DIC) and 4-(dimethylamino) pyridinium p-toluene sulfonate (DPTS). To obtain the desired monomer, a modified P-3CR was used to assemble water, an aldehyde, and an isocyanide into an α-hydroxyamide in a convergent fashion [28]. For example, hydroxy *tert*-butyl ester **H1** was obtained by the reaction of isocyanide **I1** and phenylacetaldehyde in the presence of boric acid (Fig. S9A). Subsequent deprotection of the *tert*-butyl ester provided monomer **M1** (Fig. 3a). The DIC/DPTS-mediated polycondensation of **M1** was performed in CH_2Cl_2/pyridine. The increase in solution viscosity and precipitation of urea indicated the success of the polymerization. After 24 h, polymer **P1** was recovered in 48% yield after precipitation of the CH_2Cl_2 solution into methanol ($M_n = 11.7$ kDa and $Đ = 1.58$). The polymer structure was verified by NMR spectroscopy (Fig. S15A) and MALDI-TOF-MS (Fig. 4). In this MALDI-TOF-MS spectrum, each peak was separated by 263 Da, which was consistent with the calculated molar mass of the repeating unit of **P1**. However, we could not

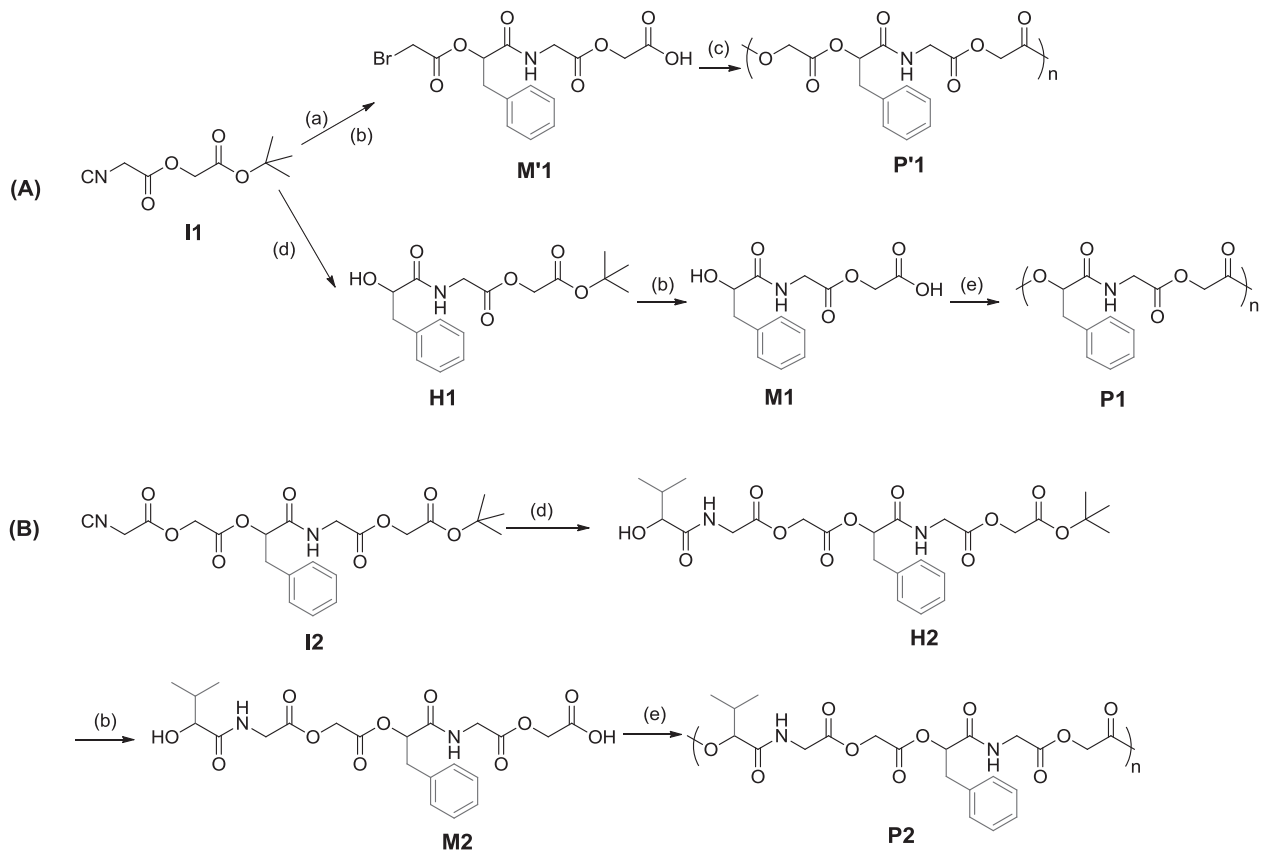

Scheme 4 Sequence-defined periodic poly(ester-amide-ester)s via polycondensation. Reagents and conditions: **a** bromoacetic acid, aldehyde, and water, room temperature, 24 h; **b** CH_2Cl_2/TFA (v/v = 3:1), room temperature, 3 h; **c** K_2CO_3, DMF, room temperature, 4 h; **d** boric acid, aldehyde, DMF, room temperature, 24 h; and **e** DPTS and DIC, CH_2Cl_2 (containing 5–6% pyridine), room temperature, 24 h

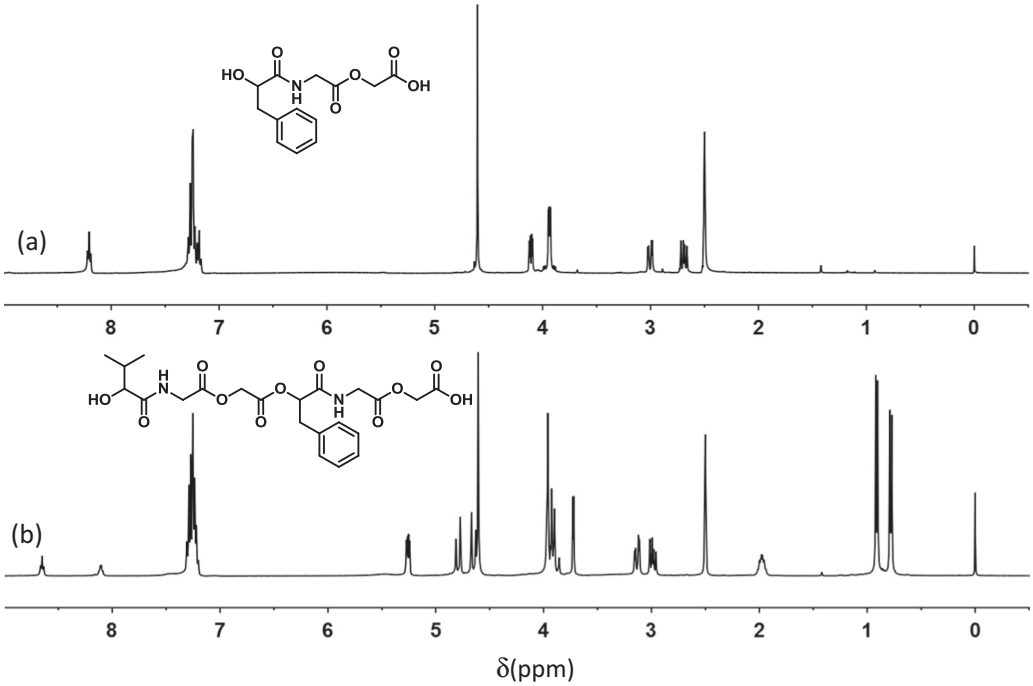

Fig. 3 ^{1}H NMR spectra of **a M1** and **b M2** in DMSO-d_6

determine the exact end groups of the polymer, as reported in the literature [29].

Furthermore, following a similar two-step reaction and starting from **I2**, we could synthesize another monomer (**M2**) with a longer sequence. Both **H2** and **M2** were characterized by NMR spectroscopy (Figs. S9 and S10 and Fig. 3b). The polymerization of **M2** under conditions similar to those used for **M1** afforded polymer **P2** (M_n = 11.1 kDa and $Đ$ = 1.22, Figs. S14–S16).

Thermal properties of the sequence-defined oligo/poly(ester-amide-ester)s

The thermal properties of **O1**, **O2**, **O3**, **O′3, P′1**, **P1**, and **P2** were investigated by TGA (Figs. S17 and S18) and DSC (Fig. 5). The collected data are summarized in Table 1. The TGA thermograms of the oligomers all exhibited a two-stage weight loss process. The first stage, which started at ~170 °C, corresponds to the release of isobutene due to the pyrolysis of the *tert*-butyl ester groups. The calculated percentages of weight loss according to the TGA data were in good accordance with the theoretical values. The second stage was from the decomposition of the ester and amide linkages. Polymers **P′1**, **P1**, and **P2** are more thermally stable than the corresponding oligomers, and they only displayed a one-stage pyrolysis process, and that could be attributed to backbone decomposition. The T_d of **P1** (T_d = 289.1 °C) was much higher than that of **P2** (T_d = 255.4 °C), although they have similar molecular weights and backbone structures. A possible reason is the differences associated with the presence of benzyl groups in **P1** and isopropyl groups in **P2**.

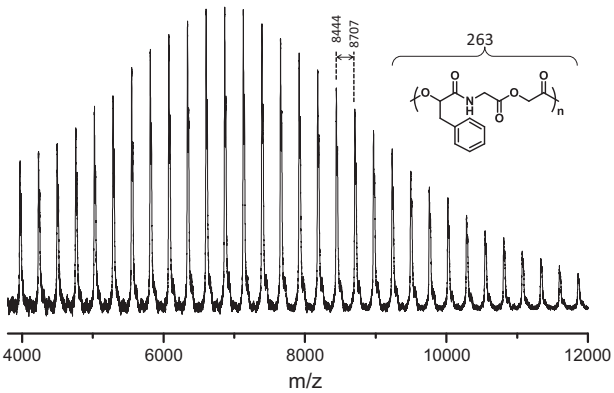

Fig. 4 MALDI-TOF-MS spectrum of **P1**

The DSC thermograms revealed that all the oligomers and polymers are amorphous and have different glass-transition temperatures. For the oligomers, T_g increased with molar mass, increasing from **O1** (T_g = 1.6 °C), **O2** (T_g = 17.6 °C) to **O3** (T_g = 22.4 °C). **O3** and **O′3** had the same backbone length, but the T_g of **O′3** (37.0 °C) was ~15 °C higher than that of **O3**, which was ascribed to the internal plasticization of the long alkyl side-chain in **O3**. The three polymers all displayed higher T_g values than those of the oligomers due to their higher molecular weights. **P′1** and **P1** had similar T_g, values, and that of **P2** was much higher (T_g = 90.4 °C). Since **P1** and **P2** had similar

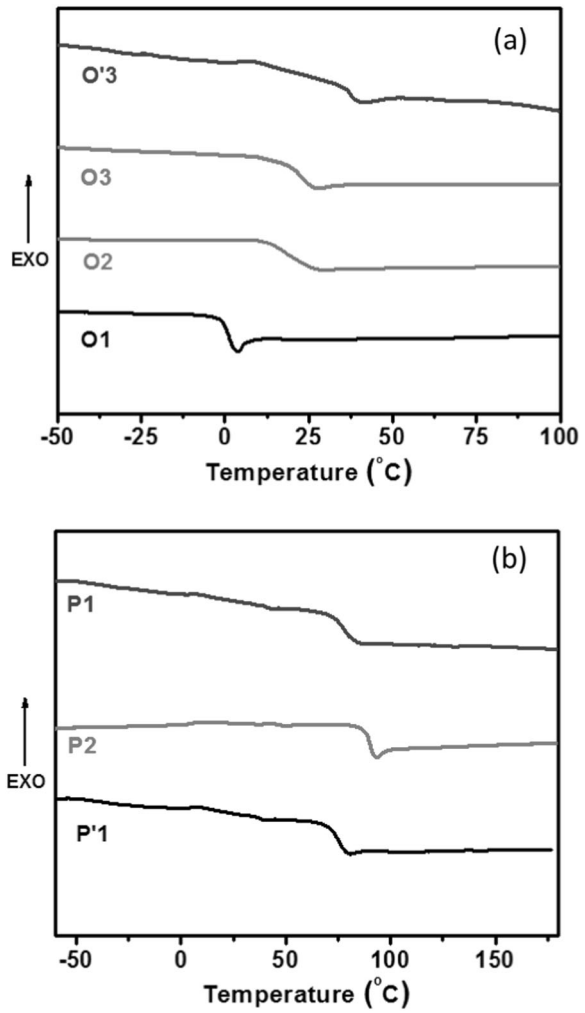

Fig. 5 DSC thermograms of a **O1–O3**, and **O′3** as well as **b P′1**, **P1**, and **P2**

molecular weights, one possible reason for the lower T_g of **P1** relative to that of **P2** is the large dispersity of **P1**. To exclude this, we fractionated **P1** into three portions with different molecular weights and narrow dispersities, and their DSC thermograms were also measured (Fig. S19). The low-molecular-weight sample exhibited a T_g at 70.3 °C ($M_n = 2.8$ kDa, $Đ = 1.17$), and this value increased with increasing molecular weight to 72.1 °C ($M_n = 6.5$ kDa, $Đ = 1.10$) and 78.1 °C ($M_n = 11.2$ kDa, $Đ = 1.08$). This trend is consistent with the well-known dependence of T_g on molecular weight. Hence, the lower T_g of **P1** can be attributed to the difference between the pendent benzyl and isopropyl groups in **P1** and **P2**.

Conclusion

We developed an efficient and straightforward strategy for the synthesis of uniform, sequence-defined oligo (ester-amide-ester)s via sequential nucleophilic substitution reactions and P-3CR. Through the judicious selection of the aldehyde, we could obtain uniform oligomers composed of α-hydroxy acid and α-amino acid monomers with ordered side chains. Iterating this process could further improve the synthetic efficiency and was more suitable for the synthesis of uniform, symmetrical, long-chain oligomers. In addition, we tested two methods for preparing periodic poly(ester-amide-ester)s through polycondensations. The intermolecular nucleophilic substitution only gave low-molecular-weight polymers, while the DIC/DPTS-mediated polycondensation of α,ω-hydroxy carboxylic acids with sequence-defined oligo (ester-amide-ester)s afforded high-molecular-weight polymers. All the oligomers and polymers synthesized via this de novo design featured unique backbone structures composed of α-hydroxy acids and α-amino acids with programmably installed side chains.

Acknowledgements This work was supported in part by the National Natural Science Foundation of China (Nos 21534001 and 21871014).

Compliance with ethical standards

Conflict of interest The author declares that he has no conflict of interest.

Publisher's note Springer Nature remains neutral with regard to jurisdictional claims in published maps and institutional affiliations.

References

1. Lutz JF, Lehn JM, Meijer EW, Matyjaszewski K. From precision polymers to complex materials and systems. Nat Rev Mater. 2016;1:16204.
2. Lutz JF, Ouchi M, Liu DR, Sawamoto M. Sequence-controlled polymers. Science. 2013;341:1238149.
3. Lutz JF. Defining the field of sequence-controlled polymers. Macromol Rapid Commun. 2017;38:12.
4. Ouchi M, Sawamoto M. Sequence-controlled polymers via reversible-deactivation radical polymerization. Polym J. 2018; 50:83–94.
5. Solleder SC, Schneider RV, Wetzel KS, Boukis AC, Meier MAR. Recent progress in the design of monodisperse, sequence-defined macromolecules. Macromol Rapid Commun. 2017;38:1600711.
6. Soejima T, Satoh K, Kamigaito M. J Main-chain and side-chain sequence-regulated vinyl copolymers by iterative atom transfer radical additions and 1:1 or 2:1 alternating radical copolymerization. Am Chem Soc. 2016;138:944–54.
7. Grate JW, Mo KF, Daily MD. Triazine-based sequence-defined polymers with side-chain diversity and backbone-backbone interaction motifs. Angew Chem Inter Ed. 2016;55:3925–30.
8. Hibi Y, Ouchi M, Sawamoto M. A strategy for sequence control in vinyl polymers via iterative controlled radical cyclization. Nat Commun. 2016;7:11064.
9. Wu YH, Zhang J, Du FS, Li ZC. Dual sequence control of uniform macromolecules through consecutive single addition by selective passerini reaction. ACS Macro Lett. 2017;6:1398–403.
10. Ji YX, Zhang LQ, Gu X, Zhang W, Zhou NC, Zhang ZB, et al. Sequence-controlled polymers with furan-protected maleimide

as a latent monomer. Angew Chem Inter Ed. 2017;56: 2328–33.
11. Kametani Y, Sawamoto M, Ouchi M. Control of the alternating sequence for N-Isopropylacrylamide (NIPAM) and methacrylic acid units in a copolymer by cyclopolymerization and transformation of the cyclopendant group. Angew Chem Inter Ed. 2018;57:10905–9.
12. Nowalk JA, Fang C, Short AL, Weiss RM, Swisher JH, Liu P, et al. Sequence-controlled polymers through entropy-driven ring-opening metathesis polymerization: theory, molecular weight control, and monomer design. J Am Chem Soc. 2019;141:5741–52.
13. Li J, Stayshich RM, Meyer TY. Exploiting sequence to control the hydrolysis behavior of biodegradable PLGA copolymers. J Am Chem Soc. 2011;133:6910–3.
14. Schmidt B, Fechler N, Falkenhagen J, Lutz JF. Controlled folding of synthetic polymer chains through the formation of positionable covalent bridges. Nat Chem. 2011;3:234–8.
15. Altintas O, Barner-Kowollik C. Single chain folding of synthetic polymers by covalent and non-covalent interactions: current status and future perspectives. Macromol Rapid Commun. 2012;33:958–71.
16. Rosales AM, Segalman RA, Zuckermann RN. Polypeptoids: a model system to study the effect of monomer sequence on polymer properties and self-assembly. Soft Matter. 2013;9:8400–14.
17. Nielsen PE. Peptide nucleic acid. a molecule with two identities. Acc Chem Res. 1999;32:624–30.
18. Horne WS, Gellman SH. Foldamers with heterogeneous backbones. Acc Chem Res. 2008;41:1399–408.
19. Fonseca AC, Gil MH, Simões PN. Biodegradable poly(ester amide)s - a remarkable opportunity for the biomedical area: review on the synthesis, characterization and applications. Prog Polym Sci. 2014;39:1291–311.
20. Basu A, Kunduru KR, Katzhendler J, Domb AJ. Poly(α-hydroxy acid)s and Poly(α-hydroxy acid-co-α-amino acid)s derived from amino acid. Adv Drug Deliv Rev. 2016;107:82–96.
21. Winnacker M, Rieger B. Poly(ester amide)s: recent insights into synthesis, stability and biomedical applications. Polym Chem. 2016;7:7039–46.
22. Shi CX, Guo YT, Wu YH, Li ZY, Wang YZ, Du FS, et al. Synthesis and controlled organobase-catalyzed ring-opening polymerization of morpholine-2,5-dione derivatives and monomer recovery by acid-catalyzed degradation of the polymers. Macromolecules. 2019;52:4260–9.
23. Llevot A, Boukis AC, Oelmann S, Wetzel K, Meier MAR. An update on isocyanide-based multicomponent reactions in polymer science. Top Curr Chem. 2017;375:66.
24. Koopmanschap G, Ruijter E, Orru RVA. Isocyanide-based multicomponent reactions towards cyclic constrained peptidomimetics. Beilstein J Org Chem. 2014;10:544–98.
25. Bonne D, Dekhane M, Zhu JP. Mild oxidative one-carbon homologation of aldehyde to amide. J Am Chem Soc. 2005; 127:6926–7.
26. Moore JS, Stupp SI. Room-temperature polyesterification. Macromolecules. 1990;23:65–70.
27. Pirrung MC, Das Sarma K. Aqueous medium effects on multicomponent reactions. Tetrahedron. 2005;61:11456–72.
28. Sravan Kumar J, Jonnalagadda SC, Mereddy VR. An Efficient Boric acid-mediated preparation of α-hydroxyamides. Tetrahedron Lett. 2010;51:779–82.
29. Stayshich RM, Meyer TY. New insights into Poly(lactic-co-glycolic acid) microstructure: using repeating sequence copolymers to decipher complex NMR and thermal behavior. J Am Chem Soc. 2010;132:10920–34.